CONDITIONS FOR ISOSCALING IN NUCLEAR REACTIONS

M. B. Tsang, W.A. Friedman[a], C.K. Gelbke, W.G. Lynch, G. Verde, H.S. Xu

In a recent survey of heavy ion induced reactions, isoscaling appears to be manifested in a variety of nuclear reactions including deeply inelastic collisions, evaporation and multifragmentation over a wide range of incident energies [1]. In this report, we will perform a comprehensive exploration of many reactions and examine conditions under which isoscaling is observed and others where it is not. We will also demonstrate how isoscaling can be restored even when two systems have different temperatures.

1 Deeply Inelastic Collisions

In the 1970's, the Deeply Inelastic Collision (DIC) phenomenon was discovered when heavy ions were used to bombard heavy targets in an effort to create superheavy elements [4,5]. Products from the DIC exhibit characteristics which can partly be attributed to compound nuclei decay and partly to multinucleon transfer reactions depending on the incident energy and detection angles. In ref. [1] the isotope yield ratios of ^{16}O + ^{232}Th and ^{16}O + ^{197}Au reactions at incident energy of 137 MeV and $\theta = 40^o$ have been found to exhibit isoscaling behavior. From the literature, we have selected four additional systems to illustrate the compliance or noncompliance of the scaling behavior in DIC . Each pair of the chosen reactions use the same projectile at the same incident energy and detect the isotopes at the same laboratory angles. The main differences are the targets. Figure 1 shows the relative isotope ratios, $R_{21}(N,Z)$ for the four systems: a.)^{16}O + ^{232}Th [4] and ^{16}O + ^{197}Pb [5] at incident

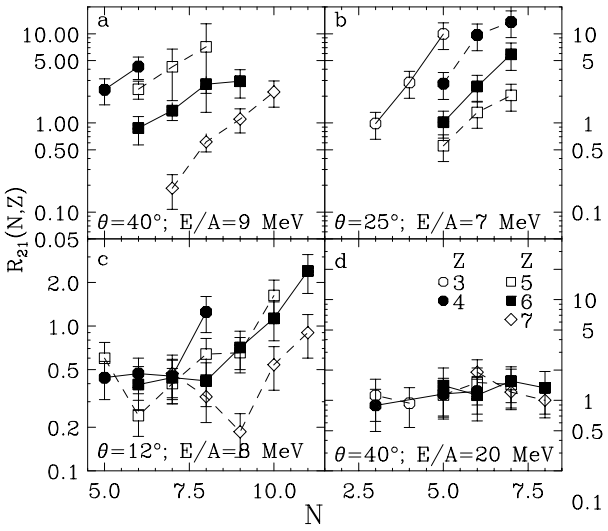

Figure 1: Relative isotope ratios for four systems: a.)^{16}O + ^{232}Th [10] and ^{16}O + ^{197}Pb [11] at incident energy of 137 MeV and $\theta = 40^o$ (upper left panel). b.) ^{14}N + ^{100}Mo and ^{14}N + ^{92}Mo at 97 MeV and $\theta = 25^o$ [10] (upper right panel). c.) ^{22}Ne + ^{232}Th and ^{22}Ne + ^{94}Zr at 173 MeV and $\theta = 12^o$ [10] (lower left panel) and d.) ^{16}O + ^{232}Th and ^{16}O + ^{197}Au at 315 MeV and $\theta = 40^o$ [11] (lower right panel).

energy of 137 MeV and $\theta = 40^o$ (upper left panel), b.) ^{14}N + ^{100}Mo and ^{14}N + ^{92}Mo at 97 MeV and $\theta = 25^o$ (upper right panel) [4], c.) ^{22}Ne + ^{232}Th and ^{22}Ne + ^{94}Zr at 173 MeV and $\theta = 12^o$ [4] (lower left panel), and d.) ^{16}O + ^{232}Th and ^{16}O + ^{197}Au at 315 MeV and $\theta = 40^o$ (lower right panel) [5]. Isotopes of the same elements are plotted with the same symbols, using open circles, closed circles, open square, closed squares, and open diamonds for Z=3, 4, 5, 6, and 7, respectively. The solid and dotted lines connect isotopes of the same elements (solid lines for even Z element and dashed line for odd Z elements). Scaling behavior consistent with

the equation

$$R_{21}(N,Z) = Y_2(N,Z)/Y_1(N,Z) = C \cdot \exp(N \cdot \alpha + Z \cdot \beta) \quad (1)$$

is observed for the isotope ratios plotted in the upper panels. When the product nuclei are detected at very forward angles, such as the isotope ratios from the ^{22}Ne induced reactions shown in the lower left panel, scaling is not observed. When the incident energy is raised to 20 MeV per nucleon, target dependence is much weaker than at lower energies [11] and production of isotopes at forward angles is consistent with fragmentation of the projectile and shows no target dependence. In that case, $\alpha = 0, \beta = 0$ and $R_{21}(N,Z) \approx 1$ is observed (lower right panel).

Figure 1 summarizes that isotopic scaling is reasonably well respected at low incident energies ($E/A < 10MeV$) and at angles backward of the grazing angles but poorly respected at forward angles. The situation at higher energies is not clear. Isoscaling may have been observed with very small values of α and β. The positive observation of isoscaling can be understood as follows: Backward of the grazing angles, it is often assumed that equilibrium is established between the orbiting projectile and target. In such cases, the isotopic yields follow the "Q_{gg}-systematics"[4,5], in which the primary isotope yield of the projectile-like fragment depends mainly on the Q-value of the mass transfer and can be approximated by

$$Y(N,Z) \propto \exp((M_P + M_T - M'_P - M'_T)/T) \quad (2)$$

where M_P and M_T are the initial projectile and target masses, and M'_P and M'_T are the final masses of the projectile- and target-like fragment. Here, T has a natural interpretation as the temperature, but is not always assumed to be so. Applying charge and mass conservation, and expressing explicitly only the terms that depend on N and Z, one can write $R_{21}(N,Z)$ as

$$R_{21}(N,Z) \propto \exp[(BE(N_2 - N, Z_2 - Z) - BE(N_1 - N, Z_1 - Z))/T], \quad (3)$$

where Z_i and N_i are the total proton and neutron number of reaction i. BE is the binding energy of a nucleus. Expanding the binding energies in Taylor series, one obtains an expression of the form

$$BE(N_2 - N, Z_2 - Z) - BE(N_1 - N, Z_1 - Z) \approx a \cdot Z + b \cdot N + c \cdot Z^2 + d \cdot N^2 + e \cdot ZN, \quad (4)$$

where $a, b, c, d,$ and e are constants from the Taylor expansion. Evaluating Eq. 4 within the context of a liquid drop model, one finds that the second order terms are of the order (1/A), where A is the mass number, relative to the first order terms. The leading order parameters, a and b can be interpreted as the differences of the neutron and proton separation energies for the two compound systems, i.e. $a = -\Delta s_n$ and $b = -\Delta s_p$. Equation 3 can then be approximated as

$$R_{21}(N,Z) \propto \exp[(-\Delta s_n \cdot N - \Delta s_p \cdot Z)/T]. \quad (5)$$

Eq. 5 confirms the earlier studies which showed that the symmetry contribution in Δs_n of the various isotopes associated with the same element, is approximately linear in the number of neutrons transferred. Similarly, Δs_n shows a linear dependence on the charge transferred due to Coulomb-barrier effects [5,6]. Comparison of Eqs. 1 and 5 reveals that the difference in the average separation energies, $\Delta s_n/T$ and $\Delta s_p/T$, plays a corresponding role to the fitting parameters of α and β. From the binding energy expansion in Eq. 4, one expects that Eq. 5 becomes less accurate and eventually breaks down leading to a failure in isoscaling when the range of fragment masses considered becomes large.

2 Compound nucleus decay

The scaling behavior for fragments evaporated from an excited compound nucleus has been discussed in ref. [1]. The measured isotope ratios for $^4He + ^{116}Sn$ and $^4He + ^{124}Sn$ collisions at $E/A = 50MeV$ [7] are plotted in Figure 2 using the same convention of Figure 1. At back angles ($\theta = 160^o$, left panel), the isotope ratios

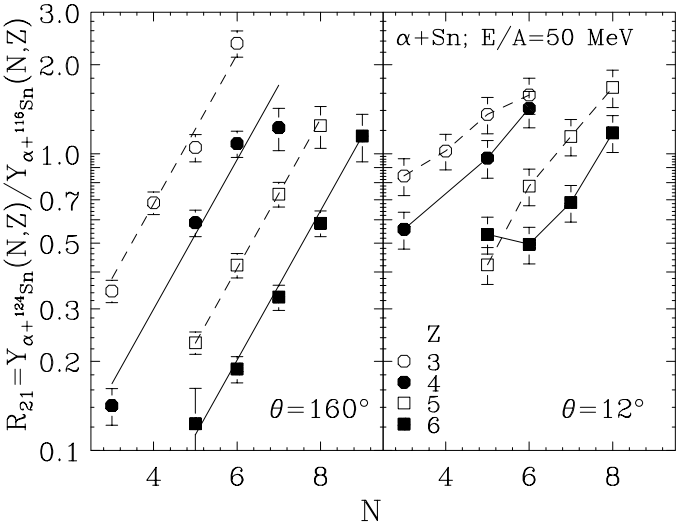

Figure 2: Relative isotope (Z=3-6) ratios for $^4He + ^{116}Sn$ and $^4He + ^{124}Sn$ systems emitted at backward (left panel) and forward angles (right panel). See Figures 1 and 2 for symbol conventions.

of different elements have similar slopes and adjacent elements are separated nearly equi-distance from each other, typical behavior of isoscaling as evidenced by the best fit solid and dashed lines. However, at forward angles ($\theta = 12^o$) where contributions from pre-equilibrium processes become significant, isoscaling is not well respected as shown in the right panel. Not only do different elements have different slopes but also the distances between adjacent isotones vary greatly [7]. In general, there is a tendency for the slope to become steeper as the fragment mass is increased, consistent with the heavier elements emitted at lower temperature. However for the carbon isotope yields, the trend is actually not monotonic with N, indicating a clear failing of isoscaling. More detailed discussions on the forward angle data can be found in Ref. [7] suggesting that the failure of isoscaling may arise from non-equilibrium emission.

The origin of isoscaling for evaporation process follows similar derivations involving the expansion of the binding energies in the Taylor series as described in previous section, resulting in a formula similar to Eq. 5.

$$R_{21}(N,Z) \propto \exp[(-\Delta s_n + \Delta f_n^*) \cdot N - (\Delta s_p + \Delta f_p^* + \Delta\Phi) \cdot Z)/T]. \quad (6)$$

where f_n^* and f_p^* are the neutron and proton excited free energy and Φ is the electrostatic potential at the surface of a nucleus. A full derivation of Eq. 6 can be found in Ref. [1].

3 Multifragmentation Process

The scaling phenomenon was first observed in multifragmentation process in the central $^{124}Sn + ^{124}Sn$ and $^{112}Sn + ^{112}Sn$ collisions[2] as demonstrated in previous articles. To obtain guidance of how the nuclei yield ratios may be systematized, we examine the dependence of the isotopic yields within the equilibrium limit of the Grand-Canonical Ensemble [8-10]. In this case predictions for the observed isotopic yield are governed by both the neutron and proton chemical potentials, μ_n and μ_p and the temperature T_i, plus the individual binding energies, $BE(N,Z)$, of the various isotopes [9,10].

$$Y_i(N,Z,T_i) = F_i(N,Z,T_i) \cdot \exp(N \cdot \mu_n/T_i + Z \cdot \mu_p/T_i) \cdot \exp(BE(N,Z)/T_i) \quad (7)$$

The factor $F_i(N,Z,T_i)$ includes information about the secondary decay from both particle stable and particle unstable states to the final ground state yields. If the two reactions have the same temperature, ($T_i = T$) the binding energy terms in Eq. (9) cancel out. If one further assumes that the influence of secondary decay on the yield of a specific isotope is similar for the two reactions, i.e. $F_1(N,Z,T) \approx F_2(N,Z,T)$, then we obtain an equation in the same form as Eq. (1):

$$R_{21}(N,Z) = C \cdot \exp(N \cdot \Delta\mu_n/T + Z \cdot \Delta\mu_p/T) \quad (8)$$

where $\alpha = \Delta\mu_n/T$ and $\beta = \Delta\mu_p/T$ reflect the differences between the neutron and proton chemical potentials for the two reactions and C is an overall normalization constant. $\Delta\mu_n$ and $\Delta\mu_p$ correspond to Δs_n and Δs_p of Eq. 5. Simulations adopting microcanonical and canonical [3] multifragmentation models show that Eq. 8 is respected. Recent SMM model calculations [11] indicate that μ_n and s_n are closely related ($\mu_n \approx -s_n + f_n^*$) for $0 \leq T \leq 3MeV$, where the decay configurations are mainly binary, but the connection between μ_n and s_n becomes increasingly weak as the role of multifragment decay configurations becomes important. These calculations also verify the insensitivities of isoscaling to the effect of sequential decays [3].

4 Mixed Systems

The isoscaling described by Eq. 1 relies on the emission mechanisms for the fragments in each reaction being described statistically with some common effective temperature and that distortions from secondary decays cancel[1,2,3,12,13]. The exhibition of the systematic trends does not imply that both reacting systems proceed with the same reaction mechanism. This point was demonstrated in Ref. [14] where isotopic yields of fragments produced in central $Au + Au$ multifragmentation process at $E/A = 35MeV$ [15] can be related approximately via isoscaling to those produced in lower multiplicity evaporation process produced in $Xe + Cu$ reactions at $E/A = 30MeV$[16]. Isoscaling arises because the temperatures for the two reactions are nearly the same i.e. $T_1 \approx T_2$, [17] even though the emission mechanisms in the two reactions differ significantly [15,16].

For reactions which differ mainly in temperatures, isoscaling is also destroyed because the binding energy terms in Eq. 7 do not cancel even if the effect of sequential decays can be neglected.

$$R_{21}(N,Z) = C \cdot \exp(N \cdot \alpha' + Z \cdot \beta') \exp(BE/T_2 - BE/T_1) \quad (9)$$

where α'=$\alpha - k\mu_{n2}$ and β'=$\beta - k\mu_{p2}$; $k = 1/T_1 - 1/T_2$. While the new scaling parameters α' and β' are related to α and β, they do not have simple physics interpretations. The left panel of Figure 3 shows the R_{21} ratios extracted from isotope yields of $^{124}Sn + ^{124}Sn$ and $^{4}He + ^{124}Sn$. There is no observable scaling in these systems with different temperatures. Isoscaling could be restored if $R_{21}(N,Z)$ in Eq. 9 is multiplied by the Boltzmann factor with binding energy and temperatures, $\exp(k * BE(N,Z))$. Previous studies suggest that the temperature of the multifragmentation reaction of $^{124}Sn + ^{124}Sn$ collision is about 5 MeV [18] and the temperature of the evaporation reaction of $^{4}He + ^{124}Sn$ is about 3 MeV [7], we obtain $k \approx 0.12$. In Figure 3, $R_{21}(N,Z)\exp(0.12 * BE)$ obtained from the same data plotted in the left panel exhibit very nice systematic behavior shown in the right panel. The restored isoscaling is clearly demonstrated by the dashed and solid lines which are the best fits through the data points with $\alpha' = 0.939$.

Currently, most temperature measurements depend on selected isotope yields e.g. the T_{iso}(HeLi) depends on the yields of ^{3,4}He and ^{6,7}Li [19,20] and T_{iso}(CLi) relies on the yields of ^{11,12}C and ^{6,7}Li [19]. Discrepancies in temperature measurements have been observed between T_{iso}(HeLi) and T_{iso}(CLi) [19]. Furthermore, temperatures derived from excited states (T_{ex}) disagree with isotope yield temperatures (T_{iso}) obtained from central collisions at incident energy greater than 35 MeV [19,20]. Such discrepancies could arise if

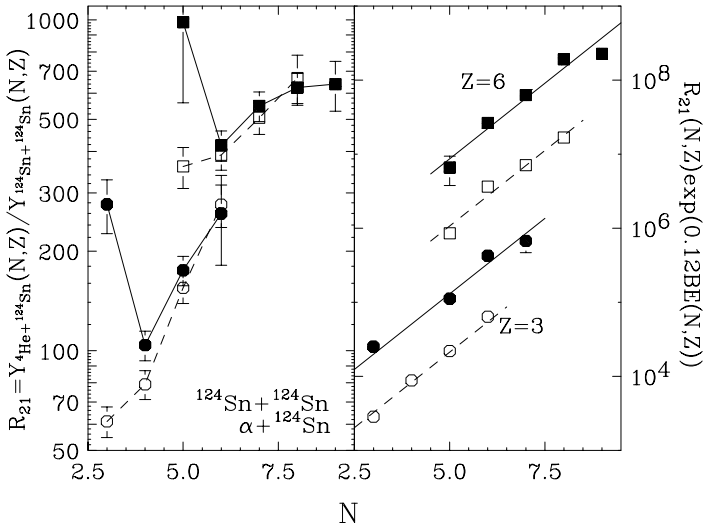

Figure 3: Left panel: Disappearance of isoscaling in reactions with different temperature. Right panel: Isoscaling is restored if the binding energy terms in the isotope ratio is corrected for the temperature difference. See Eq. 9.

the light charged particles with $Z \leq 2$ are emitted early and/or the emitting sources are not thermalized [16]. With the temperature corrected isoscaling (Eq. 9), the internal consistency of the temperature measurements and the degree of thermalization as a function of incident energy can be investigated further using all the isotopes measured instead of selected isotopes.

In summary, we have surveyed many reactions with different reaction mechanisms. We found that isoscaling occurs if both reactions can be described by statistical reaction mechanisms and that the temperatures of both reactions are nearly the same. However, isoscaling does not yield any information about the reaction mechanisms. In order to draw correct conclusions from isotopic measurements, it is therefore absolutely essential to obtain additional experimental information that elucidates the underlying reaction mechanism. If the temperatures for both reactions are different, isoscaling can be restored with appropriate temperature corrections.

The non-equilibrium reactions we have studied at forward angles show that isoscaling is not universally respected. However, it is conceivable that isoscaling could be accidentally obtained in non-equilibrium reactions. Thus, at present we can only conclude that isoscaling is a necessary but not a sufficient condition for equilibrium processes.

This work was supported by the National Science Foundation under Grant Nos. PHY-95-28844 and PHY-96-05140.

a: Department of Physics, University of Wisconsin, Madison, WI 53706

References

1. M.B. Tsang, W.A. Friedman, C.K. Gelbke, W.G. Lynch, G. Verde, H. Xu, Phys. Rev. Lett. 86, 5023 (2001).
2. H.S. Xu, et al., Phys. Rev. Lett. 85, 716 (2000).
3. W.P. Tan et al., MSUCL1198 (2001).
4. M.B. Tsang et al., MSUCL1203 (2001).
5. V.V. Volkov, Phys. Rep. 44, 93, (1978) and references therein.
6. C.K. Gelbke et. al., Phys. Rep. 42, 311 (1978) and references therein.
7. J.P. Bondorf, F. Dickmann, D.H.E. Gross and P.J. Siemens, J.de Phys. C6-145 (1971).
8. J. Brzychczyk et al., Phys. Rev. C47, 1553 (1993).
9. A.Z. Mekjian, Phys. Rev. C17, 1051 (1978).
10. J. Randrup and S.E. Koonin, Nucl. Phys. A 356, 223 (1981);
11. S. Albergo, S. Costa, E. Costanzo, A.Rubbino, Nuovo Cimento A 89, 1 (1985).

12. S.R. Souza, W.P. Tan, R. Donangelo, C.K. Gelbke, W.G. Lynch, M.B. Tsang, Phys. Rev. C62, 064607 (2000).
13. Y. Murin et al., Europhys. Lett. 34, 337 (1996); Y. Murin et al., Physca Scripta 56, 137 (1997).
14. O.V. Lozhkin et al., Phy. Rev. C 46, 1996 (1992) and references therein.
15. M.B. Tsang et al., MSUCL1165 (2000).
16. M.J. Huang et al., Phys. Rev. Lett. 78, 1648 (1997).
17. H.F. Xi et al., Phys. Rev. C57, R462 (1998).
18. H. Xi et al., Phys. Lett. B431, 8 (1998).
19. G.J. Kunde, et al., Phys. Lett. B416, 56 (1998).
20. H.F. Xi et al., Phys. Rev. C58, R2636 (1998).
21. V. Serfling et al., Phys. Rev. Lett. 80, 3928 (1998).